

An actualistic perspective into Archean worlds – (cyano-)bacterially induced sedimentary structures in the siliciclastic Nhlazatse Section, 2.9 Ga Pongola Supergroup, South Africa

N. NOFFKE,¹ N. BEUKES,² D. BOWER,¹ R. M. HAZEN³ AND D. J. P. SWIFT¹

¹Department of Ocean, Earth and Atmospheric Sciences, Old Dominion University, 4600 Elkhorn Avenue, Norfolk, VA 23529, USA

²Department of Geology, University of Johannesburg, 2006 Auckland Park, Johannesburg, South Africa

³Geophysical Laboratory, Carnegie Institution, 5251 Broad Branch Road, NW, Washington DC 20015, USA

ABSTRACT

Extensive microbial mats colonize sandy tidal flats that form along the coasts of today's Earth. The microbenthos (mainly cyanobacteria) respond to the prevailing physical sediment dynamics by biostabilization, baffling and trapping, as well as binding. This biotic–physical interaction gives rise to characteristic microbially induced sedimentary structures (MISS) that differ greatly from both purely physical structures and from stromatolites. Actualistic studies of the MISS on modern tidal flats have been shown to be the key for understanding equivalent fossil structures that occur in tidal and shelf sandstones of all Earth ages. However, until now the fossil record of Archean MISS has been poor, and relatively few specimens have been found.

This paper describes a study location that displays a unique assemblage with a multitude of exceptionally preserved MISS in the 2.9-Ga-old Pongola Supergroup, South Africa. The 'Nhlazatse Section' includes structures such as 'erosional remnants and pockets', 'multidirected ripple marks', 'polygonal oscillation cracks', and 'gas domes'. Optical and geochemical analyses support the biogenicity of microscopic textures such as filamentous laminae or 'orientated grains'. Textures resembling filaments are lined by iron oxide and hydroxides, as well as clay minerals. They contain organic matter, whose isotope composition is consistent with carbon of biological origin.

The ancient tidal flats of the Nhlazatse Section record four microbial mat facies that occur in modern tidal settings as well. We distinguish endobenthic and epibenthic microbial mats, including planar, tufted, and spongy subtypes. Each microbial mat facies is characterized by a distinct set of MISS, and relates to a typical tidal zone. The microbial mat structures are preserved *in situ*, and are consistent with similar features constructed today by benthic cyanobacteria. However, other mat-constructing microorganisms also could have formed the structures in the Archean tidal flats.

Received 16 November 2006; accepted 30 June 2007

Corresponding author: N. Noffke, Tel.: 1-757-683-3313; fax: 1-757-683-5303; e-mail: nnoffke@odu.edu.

INTRODUCTION

Life in the Archean eon appears to have been strange and unfamiliar. Sturdy, reef-like stromatolites colonized the earliest preserved shallow-marine palaeoenvironments, and testify to the metabolic activity of the earliest prokaryotes (e.g. Walter, 1972; Lowe, 1980; Walter *et al.*, 1980; Buick *et al.*, 1981; Beukes & Lowe, 1989; Buick, 1992; Hofmann *et al.*, 1999; Schopf, 2006). However, actualistic studies of modern stromatolites demonstrate that it is often very difficult to distinguish between biological and sedimentological processes

in the formation of stromatolitic build-ups (e.g. Reid *et al.*, 2000). Consequently, some Archean stromatolite-like structures have been ascribed to nonbiological processes (e.g. Lowe, 1994; Grotzinger & Rothman, 1996; Grotzinger & Knoll, 1999; Buick, 2001; Brasier *et al.*, 2006).

Ancient life is also preserved in the form of tiny body fossils of microbes (e.g. Knoll & Barghoorn, 1977; Awramik *et al.*, 1983; Walsh & Lowe, 1985; Schopf & Packer, 1987; Schopf, 1993; Westall *et al.*, 2001; Altermann & Kazmierczak, 2003; Knoll, 2003; Tice & Lowe, 2004). Because various geological processes can form similar but abiotic features, specific criteria

should be used to evaluate the biogenicity of textures and structures (e.g. Schopf & Walter, 1983; Buick, 1990; Brasier *et al.*, 2002, 2005, 2006; Schopf *et al.*, 2002; Schopf, 2006). Furthermore, valuable information on the former presence of prokaryotes in Archean time is provided by laboratory analyses that detect biomolecules or isotopes fractionated by biological processes in Earth's old rocks (e.g. Schidlowski *et al.*, 1983; Brocks *et al.*, 1999; Knoll, 1999; Summons *et al.*, 1999; Shen *et al.*, 2001; Ueno *et al.*, 2001; Strauss, 2003; Faure & Mensing, 2004).

Whereas most palaeontological studies on early life have focused on precipitated lithologies such as carbonate rocks or chert, fewer investigations have been conducted on siliciclastic (sandy) deposits. But sandstones formed in Archean shallow-marine basins and tidal flats also contain sedimentary structures produced by microorganisms (Noffke *et al.*, 2003b, 2006a,b). These structures have been termed 'microbially induced sedimentary structures' (MISS), and display a great variety of morphologies much different to those of stromatolites (Noffke *et al.*, 2001b). Whereas the term 'stromatolite' explicitly means 'layered rock', most MISS do not resemble a layered rock. For structures such as 'mat chips', 'multidirected ripple marks', 'erosional remnants and pockets', 'orientated grains', and many others, a new collective term is required, and thus MISS form a separate category in the classification of primary sedimentary structures *sensu* Pettijohn & Potter 1964 (Noffke *et al.*, 2001b). Microscopic analysis of MISS thin-sections may reveal filament-like textures, but body fossil preservation such as in chert is very rare (e.g. Noffke *et al.*, 2003b). MISS occur not only in Archean rocks, but have been described from equivalent palaeoenvironmental settings of all ages (Gehling, 1982, 1999, 2000; Bland, 1984; Runnegar & Fedonkin, 1992; Hagadorn & Bottjer, 1997, 1999; Schieber, 1999, 2004; Simonson & Carney, 1999; Noffke, 2000; Noffke *et al.*, 2002, 2003b, 2006a,b; Bottjer, 2005). Today, the formation of these structures can be observed and quantified in modern sandy tidal flats (review in Noffke *et al.*, 2003a). In contrast to stromatolites, MISS do not arise predominantly from syndepositional chemical precipitation and early cementation, but from mechanical interaction of microbial mats with siliciclastic sediment. Baffling and trapping causes deposition of sediment, and biostabilization (microbial sediment fixation) acts against erosion. Binding (the establishment of a mat fabrics) and growth take place during calm dynamic conditions between siliciclastic depositional episodes. MISS are distinctive structures that cannot be easily mimicked by purely physical processes.

Until now only a few specimens of MISS of Archean age have been found (Noffke *et al.*, 2003b, 2006a,b). In the 3.2-Ga-old Moodies Group, Barberton Greenstone Belt, South Africa, two 'wrinkle structures' and one 'roll-up structure' were detected in tidal flat sandstones. The 2.9 Ga Ntombe Formation, Pongola Supergroup, South Africa, preserves eight 'wrinkle structures' recording ancient microbial mats on shallow shelf deposits. The nearly isochronous shelf

sandstones of the Brixton Formation of the Witwatersrand Supergroup yielded 28 specimens of 'wrinkle structures', two specimens of 'erosional remnants and pockets', and one bedding plane displaying 'oscillation cracks'. All of these specimens are only of centimeter or decimeter scale. In thin-sections, textures that resemble degraded microbial mat fabrics are visible. Cyanobacteria have been suggested to be the constructing agents; however, no unambiguous evidence could be documented (see discussions in Noffke *et al.*, 2003b, 2006a).

As the record of MISS in Archean sandstones is so sparse, the discovery of a new section of 2.9-Ga-old rocks that contain numerous and exceptionally well-preserved MISS is noteworthy. This contribution describes that section of tidal sandstones, which is located in the Mozaan Group, Pongola Supergroup, South Africa. The location is here termed the 'Nhlazatse Section', after the nearby village Nhlazatse. Because of the outstanding preservation and the high number of the MISS, narrow biofacies zones of an ancient tidal flat can be distinguished. The same narrow biofacies zones occur in equivalent modern tidal settings. Although our actualistic approach uses Recent microbial mats as a model to interpret the fossil sedimentary structures, no conclusions are drawn here regarding the taxonomy of the ancient microbiota. Nevertheless, the findings are consistent with the presence of benthic cyanobacteria.

STUDY AREA

The Nhlazatse Section is exposed at the Wit Mfolozi River Gorge, about 70 km south-east of the town of Vryheid (Fig. 1A,B). The outcrop is located at 31°15'E and 28°10'S, on the left side of the road R34 (towards Durban). The section belongs to the Kwaaiman Member of the Sinqueni Formation, Pongola Supergroup, and comprises 46 m of conglomerates, quartzites, fine sandstones, silt- and mudstones (Matthews, 1967; Beukes & Cairncross, 1991; Beukes, 1996; Beukes *et al.*, 2002) (Fig. 2).

The base of the section is formed by 1- to 2-m-thick conglomerate bars. Above these, fine sandstone beds including small ripples indicate water depths of 1–10 cm deep. The sandstone beds alternate with mud-rich silt and fine sandstone beds that display desiccation cracks. The desiccation cracks record subaerial exposure of the ancient depositional surface. Together with decimeter-scale strata that include flaser bedding, the sedimentary structures are interpreted to record a tidal depositional environment. The tidal range might have been micro- to mesotidal (Matthews, 1967; Beukes & Cairncross, 1991; Beukes *et al.*, 2002).

Today, equivalent tidal flats can be found along the North Atlantic coast. The tidal flats are the result of the Holocene transgression, and may be overgrown by abundant microbial mats that extend over several hundreds of square kilometers. Similar to the modern situation, ancient microbial mats evidently accumulated primarily during sea level rises too. Indeed, MISS in rock successions are indicative of turning

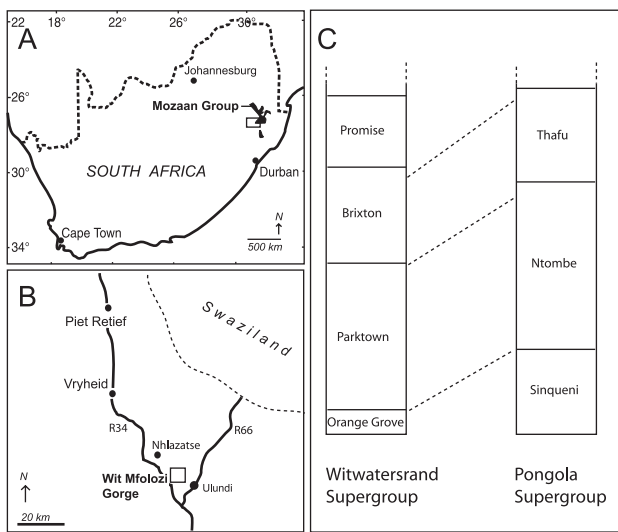


Fig. 1 Location of the siliciclastic Nhlazatse Section (Sinqueni Formation), Pongola Supergroup, South Africa. (A) The stratigraphic section belongs to the about 2.9-Ga-old Mozaan Group, which crops out in the north-eastern part of South Africa; (B) The Nhlazatse Section is exposed in the Wit Mfolozi River Gorge, about 70 km south-east of the town Vryheid. The section was named after the small village Nhlazatse close to this gorge. (C) Stratigraphic position of the Sinqueni Formation. Sandstones of the younger Ntombe Formation (Pongola Supergroup), and the Brixton Formation (Witwatersrand Supergroup) contain MISS, however, much less well preserved (Noffke *et al.*, 2003b, 2006a,b).

points of regression-transgression cycles (Noffke, 2000; Noffke *et al.*, 2003b, 2006a,b). The Nhlazatse Section records a transgressive trend as well. The lower portion of the stratigraphic succession is dominated by intertidal structures, whereas towards the top subtidal structures such as ripple marks of > 12 cm spacing become more frequent.

The rocks of the Nhlazatse section are not overprinted by strong tectonic fabrics, and experienced only a relatively low grade of metamorphism to greenschist facies (Matthews, 1967;

Beukes & Cairncross, 1991; Beukes *et al.*, 2002). Therefore, the sedimentary structures are clearly visible and little deformed. Because of the high amount of silica cement in the Nhlazatse sandstone, the MISS are better preserved than in the sandstone successions of the Ntombe Formation, Pongola Supergroup, and the Brixton Formation, Witwatersrand Supergroup. The Nhlazatse Section displays a great variety of MISS, and about 67% of all rock beds include biogenic structures. In addition, the Sinqueni Formation is somewhat older than the Ntombe and Brixton Formations (Fig. 1C).

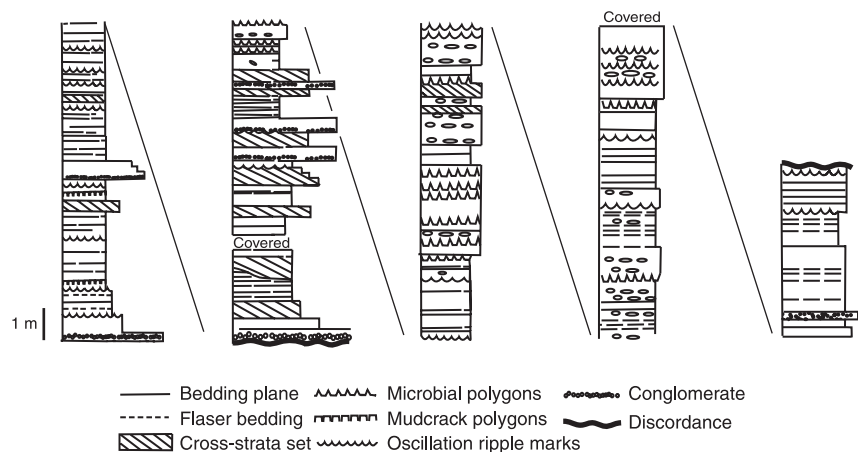
METHODS

In order to reconstruct the palaeogeographical setting of the microbial mats, we conducted a layer-by-layer survey of the stratigraphic section. The survey correlated MISS with associated physical sedimentary structures, mineral composition, bed thicknesses, and other lithological characteristics (Noffke, 2000).

In order to compare the fossil MISS with equivalent structures from modern tidal flats, we measured the geometries of the ancient structures (e.g. heights of erosional remnants, crest-to-crest distances of ripple marks, etc.). Earlier, actualistic studies defined MISS in the Recent, and quantified the processes of their formation (Noffke *et al.*, 1997; Noffke, 1998, 1999; Noffke & Krumbeyn, 1999). Ancient and modern MISS can be compared directly, because while deswelling and compaction have taken place during the lithification of the Archean deposits, sandstone composed of quartz with minimal silica cement is not significantly compacted.

One hundred and twelve MISS samples were collected, and 67 thin sections prepared. The thin sections are uncovered, and 5 μm to 25 μm thick, in order to focus microprobe measurements on small textures. Polishing, completed with 0.3 μm alumina paste, is of microprobe grade. For the optical-petrological investigations we used an Olympus BX51 microscope (Olympus America, Inc., Melville, NY, USA), as well as an Olympus

Fig. 2 The Nhlazatse Section, Pongola Supergroup, is 46 m thick, and is composed of mud-, silt-, and sandstones. The physical sedimentary structures such as desiccation cracks, shallow-water ripple marks, and flaser bedding, record wide tidal flats in a micro to mesotidal regimen. A few quartzite and conglomerate bars are intercalated, whereas precipitated lithologies are absent.



SZX 12 stereoscope, both equipped with a Q-Color 3 digital camera. Point-counting served to determine the petrological composition of the rock.

In order to evaluate the biogenicity of MISS, we conducted different geochemical analyses that have been useful for sandstone lithologies (Noffke, 2000; Noffke *et al.*, 2003b, 2006a,b). For qualitative maps of elemental composition with $\pm 2 \mu\text{m}$ resolution and quantitative point chemical analyses, a JEOL 8900 electron microprobe (JEOL Ltd., Tokyo, Japan) with five wavelength-dispersive spectrometers and an energy-dispersive spectrometer at the Carnegie Institution of Washington were employed. The analyses were performed at 15 kV with a beam current of 3000 nA on Al-coated samples (Boyce *et al.*, 2001).

Isotopic measurements of $\delta^{13}\text{C}$ were made on crushed rock in tin foil sample holders. In order to calibrate these measurements, acetate standards were run in duplicate before and after the samples. We used a Carlo Erba elemental analyser coupled to a Finnigan DeltaPlusXL continuous-flow isotope-ratio mass spectrometer (Finnigan MAT GmbH, Bremen, Germany) via a ConFlo II interface. Two procedures to evaluate potential contamination were adopted. First, we extracted rock material from the weathered surface of the MISS samples and compared the isotope data with those extracted from fresh portions of the MISS samples. These powdered samples were washed in methylene chloride to extract any soluble organic contaminants. All powdered samples were run in triplicate.

Investigations with a Raman microscope (Witec GmbH, Ulm, Germany) were performed to study the petrology of the fine-grained matrix. Five-micrometer and $30 \mu\text{m}$ thin sections were investigated using a WITec Digital Pulse scanning near-field optical microscope (AlphaSNOM, WITec ag, Littau, LU, Switzerland) with Scan Control Spectroscopy Plus. We scanned across the samples using a frequency-doubled YAG laser with wavelength 532 nm. The laser was focused through a $25\text{-}\mu\text{m}$ -diameter fibre and a $\times 20$ ocular lens. The scan speed was 4–6 s dwell time per pixel at 78 kW cm^{-2} . For facies 1, a 3 h 3 min scan over a $60 \times 30 \mu\text{m}$ area with 4 s dwell time was conducted over dark laminae at the top edge of the thin section. For facies 2, 9 h 9 min and 12 h 15 min scans over a $60 \times 30 \mu\text{m}$ areas with 6 s dwell time were conducted over dark laminae in the lower, coarser grained portion of the thin sections. The spectra generated by elemental constituents in the samples were analysed with WITtec 1.84 software.

ANCIENT MICROBIAL MAT FACIES IN THE NHLAZATSE SECTION AND THEIR MODERN COUNTERPARTS

The Nhlazatse Section represents a sandy tidal flat, in which subtidal, intertidal, and lower supratidal environments can be distinguished (Fig. 2). A great variety of exceptionally preserved MISS show that large areas of the tidal flats were overgrown by microbial mats. The microbial mats formed four

mat facies, including three subfacies. Most of the microbial sedimentary structures are preserved *in situ*. Today, similar mat facies that correspond largely to tidal zones can be observed ('biofilm-catenae' in Noffke & Krumbein, 1999; Noffke *et al.*, 2001a).

In the following sections, we describe the tidal mat facies of the Nhlazatse Section, and compare them with the biogenic structures of modern tidal flats.

The subtidal and lower intertidal zone: noncolonized by microbial mats

The subtidal and lower intertidal zones of the Nhlazatse Section do not contain any MISS. In the outcrop, mud- and siltstone beds alternate with sandstone beds. Many upper bedding planes of fine- to medium-grained sandstones display current ripple marks of about 8–12 cm crest-to-crest. The suite of sedimentary structures includes 10- to 40-cm-thick cross-strata sets, which occupy about 15% of the section. The bases of the cross-strata sets are disconformable with up to 30 cm of relief. The sandstone consists of about 95% quartz, with about 5% mica, feldspar, and heavy minerals. The quartz grains appear subangular to well rounded, and sometimes reveal dissolution margins in thin section. The degree of sorting is medium to high.

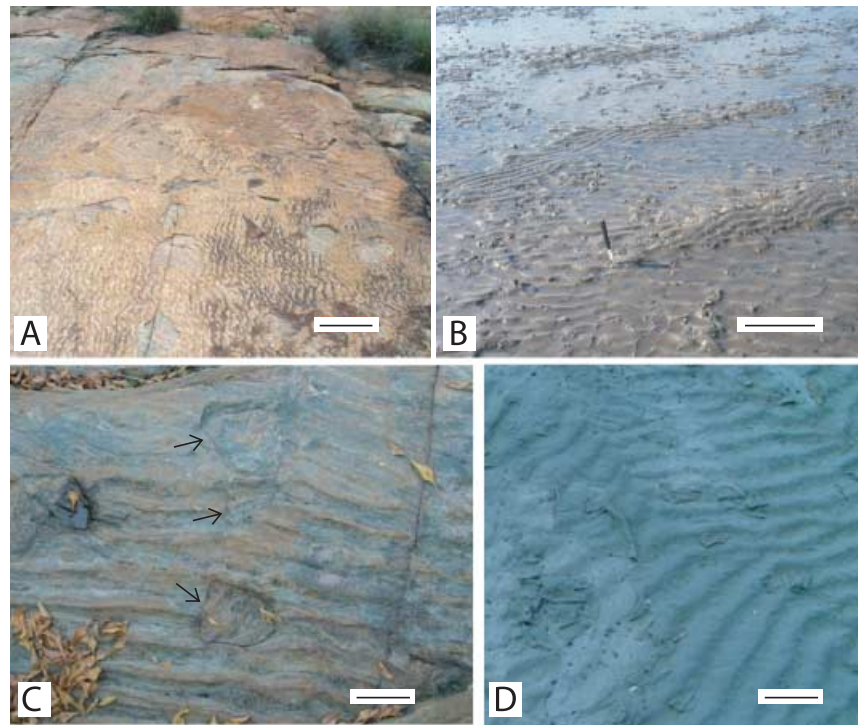
The lack of any MISS in the subtidal and lower intertidal environments of the Nhlazatse Section conforms with the distribution of microbial mats on modern tidal flats such as of Mellum Island (Noffke & Krumbein, 1999). Due to the constant hydraulic reworking of the tidal flat sands along the low water line, no mats form in these zones. Though the sediment surface of the lower intertidal zone is subaerially exposed during the ebb tide, the time periods of exposure of the sea floor are too short to permit the construction of microbial mat fabrics. Rather, the microbes only form biofilms (organic envelopes) around single mineral grains. Mostly, such organic-mineral aggregates stay in turbulent suspension, because of their low density relative to sterile grains.

The upper intertidal zone: colonized by 'endobenthic' microbial mats

The upper intertidal zone of the Nhlazatse Section is characterized by sand-, silt- and mudstone beds. Mud cracks and flaser-bedding are common and support the interpretation of an intertidal environment. The sandstones show a composition of 88–96% quartz, with associated clay, mica, feldspar and heavy minerals. As in the lower intertidal zone, the quartz grains appear subangular to well rounded, and in thin-sections sometimes show dissolution margins. The degree of sorting is medium to high.

The upper intertidal zone is characterized by MISS of endobenthic microbial mats (Fig. 3A,C). 'Endobenthic' means that the microorganisms have colonized the uppermost millimeters of the sedimentary deposits without projecting from the sandy surface. Consequently, the original morphologies of

Fig. 3 MISS in the upper intertidal zone of the Nhlazatse Section, Pongola Supergroup; and modern equivalents. Both the ancient and the Recent upper intertidal zones are colonized by 'endobenthic' microbial mats. Note that the ripple marks underneath the microbial mats are easily visible. (A) 'Multidirected ripple marks' covering a fine sandstone bed in the Nhlazatse Section; scale: 1 m. (B) In the modern tidal flats of Mellum Island, North Sea, multidirected ripple marks arise from the interference of microbial mat growth and episodic reworking events; scale: 25 cm, June 1995; (compare A, B with Figs 4 and 5). (C) In the Nhlazatse Section, three microbial mat chips (arrows) had been deposited on a rippled sandy surface; scale: 5 cm. (D) In the Recent, pieces of a microbial mat are ripped off their parent site by currents and are redeposited close-by. Such chips indicate that the sand is bound together by a cohesive microbial mat; scale: 5 cm; October 2002, Fishermans Island, Virginia, USA.



the physical surface (e.g. ripple marks) are still clearly visible. On modern tidal flats, such endobenthic mats grow in the upper intertidal zones of Mellum Island (Noffke & Krumbein, 1999) (Fig. 3B,D). Here, the microbial mats are dominated by the highly mobile cyanobacterial species *Oscillatoria limosa* (Villbrandt, 1992; Golubic & Knoll, 1999).

In both the ancient and the modern environments, endobenthic microbial mats form multidirected ripple marks, mat chips, and microsequences. Those structures will be described in the following section.

Multidirected ripple marks

In the Nhlazatse Section, 17 beds display randomly orientated ripple marks that have 2- to 8-cm crest-to-crest distances (Fig. 3A). The ripples are straight-crested oscillation or combined flow ripples with short wavelengths. On modern tidal flats, the formation of such multidirected ripple marks (Noffke, 1998) has been monitored on Mellum Island, where such ripple pattern develops in the course of a growth season (Fig. 3B).

With the increasing temperatures in spring, microbial mats start to overgrow the rippled sandy surface of the upper intertidal zone. Wind-reinforced, strong flood currents rework the ripple marks, and new ripple marks a different orientation ripple marks. However, those surface areas of the tidal flats that are covered and biostabilized by microbial mats remain unaffected by the currents; the tidal surface now displays two ripple mark directions. In the following months, each reworking event gives rise to a new generation of ripple marks that are subsequently

overgrown and stabilized by microbial mats in the period of calm dynamic conditions inbetween two events. Finally, by fall, a chaotic-like pattern of multidirected ripple marks covers the tidal flats.

In the Nhlazatse Section, the number of flooding events and the directions of the currents can be reconstructed for each multirippled rock bed surface (Fig. 4). The ancient ripple pattern records orbital velocities of about 25 cm s^{-1} and high-water depths in the order of 10–30 cm. Those values are consistent with the measurements from multidirected ripple marks of modern microbial mat settings (Noffke, 1998).

Microbial mat chips

One bedding surface includes abundant chips of lithified sediment about 1–4 cm in diameter and only up to 0.25 mm thickness (Fig. 3C). Thin sections show that the chips are composed nearly exclusively of sand grains, not of mud. Some chips are overfolded, which shows that the formerly loose sand grains must have been bound together by a coherent matrix such as a microbial mat (Pflueger & Gresse, 1996). On the modern tidal flats of Mellum Island, microbial mat chips of equivalent sizes and thicknesses are ripped off their parent mat by spring high tide currents, and the chips are scattered at random across the tidal flats (Fig. 3D).

Microsequences

Polished slabs and thin sections of MISS-bearing Nhlazatse sandstone samples display 31 layers of 2–10 mm thicknesses composed of sandstone at their bases and dark grey laminae at

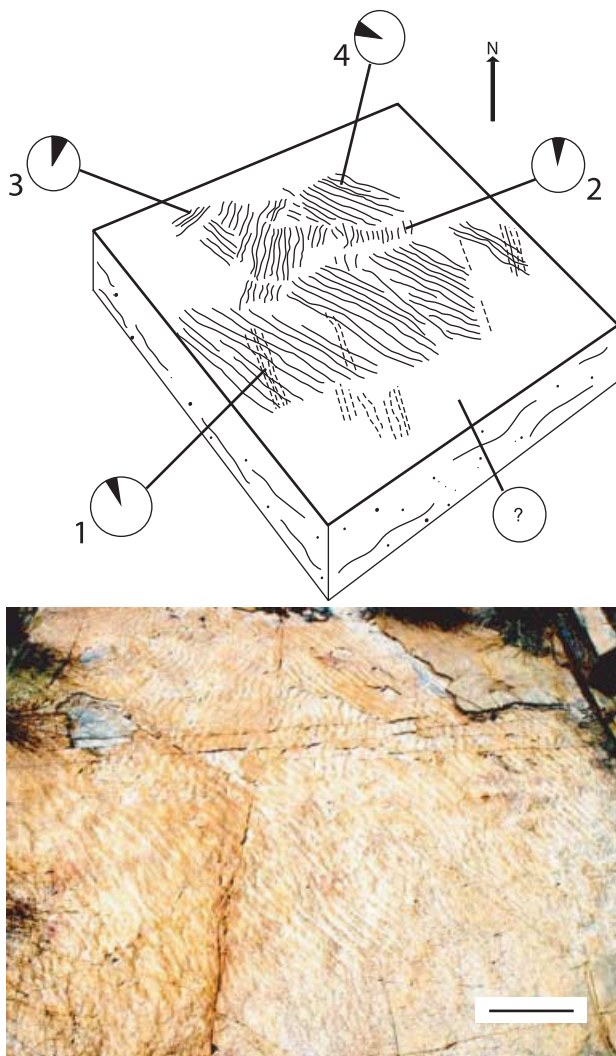


Fig. 4 Fossil multidirected ripple marks from the Nhlazatse Section, Pongola Supergroup, South Africa. View of multidirected ripple pattern exposed on a 7- to 10-cm-thick fine sandstone bed; scale: 1 m. The ripple pattern is composed of patches (or groups) of ripple marks. Each patch (or group) is characterized by one ripple crest direction as shown in the stereonets. The analysis of the pattern shows that the ripple mark groups have been formed subsequently during individual reworking events (compare Noffke, 1998). The numbers 1–4 indicate the order of formation of the ripple generation. The first generated ripple marks are least well visible, and mostly occupy the smallest area on the bedding plane. (1) 5%; (2) about 1.5%; (3) 17%; (4) 45%; (nonpreserved) 33%.

their tops (Fig. 5A). Such layers are termed ‘microsequences’ (Noffke *et al.*, 1997). In the Nhlazatse Section, the basal sandstone portion of each microsequence appears often normally graded (grain sizes range from 0.060 to 0.4 mm).

Under magnification, the laminae that form the top of each microsequence are about 80–100 μm thick, and contain particles of in average 0.02 mm grain sizes. The dark laminae themselves are composed of iron oxide (haematite), iron hydroxide (goethite), a titanium oxide, chlorite, and carbon.

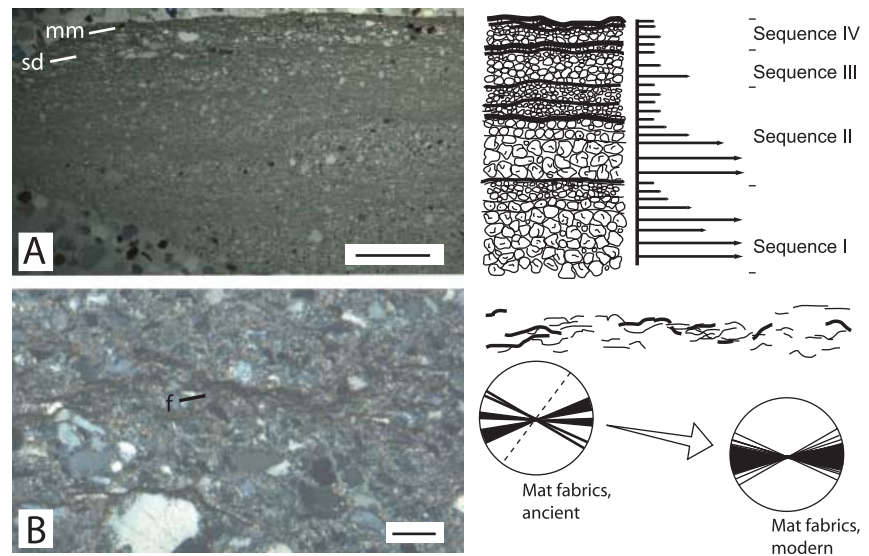
The laminae can be unconformable to each other, ranging between 0 and 15° from horizontal.

Microsequences have first been described from vertical sections of sediment cores from modern, mat-overgrown tidal deposits (Noffke *et al.*, 1997). First, sand is deposited, sometimes normally graded because of decreasing hydraulic energy (Fig. 5A, right). At a certain point, the reworking is so minimal that microbial mats can form on the sedimentary surface. Baffling and trapping of those microbial mats enrich particles of mainly silt sizes. Because of the similar grain size distributions, and of the appearances of the laminae, we assume that the dark grey laminae of the Nhlazatse Section are fossil microbial mats. Fossil microsequences also are known from the Mozaan Group (Pongola Supergroup) (e.g. Noffke *et al.*, 2003b).

Multidirected ripple marks, microbial mat chips, and microsequences are not the only clues to the former presence of microbial mats. In high magnification, thin sections show that the dark laminae are composed of ‘wavy-crinkly’ textures (Schieber, 1999) that look similar to degraded microbial mats. These laminae have a fine-grained matrix (Fig. 5B) around which many larger sand particles have grain-to-grain contact. The microscopic wavy-crinkly textures appear to be interwoven and they form a mesh-like fabric that resembles the organic network of modern microbial mats. Statistical analyses of the wavy-crinkly textures show angles of 0–45° (Fig. 5B, right). The same orientation of layers can be found in modern microbial mat layers composed of the cyanobacteria *Microcoleus chthonoplastes* and *Oscillatoria limosa*, although the modern textures are not affected by postburial compaction. Fossil textures of this kind also are known from many other tidal sandstones (Noffke, 2000; Noffke *et al.*, 2002, 2003b, 2006a,b).

Dark laminae could also be interpreted as stylolites, which are pressure solution features that result in the removal of all material in a layer except for an insoluble residue. The mineralogy of the dark laminae provides important clues. If the dark laminae are stylolites then they should be characterized by a concentration of clays and other relatively insoluble minerals. Alternatively, if they are degraded mats then clays and other insoluble minerals should be more abundant in the sandy interlayers. MicroRaman and microprobe analyses indicate that the sandy layers in between the dark laminae are composed primarily of quartz, with chlorite and mica. The laminae, however, are composed of iron oxide and hydroxide, titanium oxide, chlorite, and carbon. Those minerals frequently compose fossil microbial mat laminae in tidal sandstones from other study locations (Noffke, 2000; Noffke *et al.*, 2002, 2003b, 2006a,b). Isotope measurements also support the biogenicity of the degraded-mat textures. Fresh, unweathered laminae have 0.02–0.03 wt% carbon with $\delta^{13}\text{C}$ values of -22.77‰ to -22.95‰ in two separate analyses. By contrast, organic material concentrated from the edge of the samples has 0.04–0.05 wt% carbon with a $\delta^{13}\text{C}$ value of -20.85‰ to -21.72‰ in two separate analyses. Therefore, the interior organic matter does not appear to be a contaminant from the outside of the rock.

Fig. 5 Ancient microbial mats in fine sandstones of the Nhlazatse outcrop. (A) Thin sections perpendicular to the bedding surface microsequences composed of fine sandstone (sd) at their bases, and wavy-crinkled laminae of fossil microbial mats (mm) at their tops; scale: 1 cm. Right: this thin-section reveals four microsequences. Note that only if the current velocities become very small will a mat fabric form (binding). (B) In close-up, the laminae are composed of elongated textures (f) that form a carpet-like network; scale: 100 μm . Right: The orientations of the fossil textures forming a mat fabric correspond to those of filaments in modern microbial mats (constructed mainly by the benthic cyanobacterium *Microcoleus chthonoplastes*). The length axes of the filaments are visible. Both the fossil and the recent filaments form an angle of about 45°. The fossil microbial mats might have been compacted due to syndepositional load pressure. The laminae are composed of iron oxides and hydroxides, titanium oxides, chlorite, and carbon.



Comparable sandstone samples of other tidal sandstone successions show similar carbon isotope ratios and carbon abundances (Noffke *et al.*, 2003b, 2006a,b). Therefore we favour the interpretation of the dark laminae as degraded microbial mats. Nevertheless, stylolites remain a possible alternative interpretation.

The lower supratidal zone: colonized by epibenthic microbial mats (planar, tufted, and spongy)

The lower supratidal zone recorded in the Nhlazatse Section is also characterized by a variety of MISS and *in situ* lithified microbial mats. The ancient microbial mats were 'epibenthic'; that is, the very thick microbial mats developed atop the sedimentary surface smoothing the original physical surface so that previously formed structures such as ripple marks were not visible any more (Fig. 6A). Such microbial mats conform with the mat types developing on the modern tidal flats of Mellum Island (Noffke & Krumbein, 1999), coastal Tunisia (Noffke *et al.*, 2001a) and on the Bahamas (Hardie, 1978) (Fig. 6B). Because of the ubiquitous extracellular polymeric substances (EPS, Decho, 1990) that these microbial mats produce, somewhat different MISS are formed. The modern microbial mats are of (i) planar, (ii) tufted and (iii) spongy types.

Subfacies 1: Planar microbial mats

Planar microbial mats are abundant in the Nhlazatse Section, and they form erosional remnants and pockets, gas domes, and orientated grains.

Erosional remnants and pockets. Four sandstone beds display a morphology composed of (i) elevated, flat-topped and green-coloured surfaces of about 50–200 cm diameter, and (ii) deeper-lying, ripple-marked and sand-coloured surfaces of

similar diameters (Fig. 6C). In the modern tidal flats of Mellum Island, such a surface morphology is termed 'erosional remnants and pockets' (Gerdes *et al.*, 1993; Noffke, 1999) (Fig. 6D). Erosional remnants and pockets arise from partial erosion of a microbial mat-covered tidal sand surface.

The erosional pockets document the process of erosion starting locally from a small spot, where the microbial mat cover has been damaged. From those initial spots, erosion washes away the sand underneath the microbial mat, and finally rips off mat chips (Fig. 6E,F). Small depressions develop and expose the bare sand, where ripple marks begin to form. With continuing erosion, the depressions expand laterally to up to 25 cm depth and 2 m diameter. The fossil tidal surface in the Nhlazatse Section records those erosional processes beautifully (Fig. 7). Measurements on modern *Microcoleus chthonoplastes*-dominated mats show that currents of 60–75 cm s^{-1} are necessary to rip off a mat chip. The chips are transported up to 200 m before they become too small to be recognized macroscopically on the tidal surface. Often, mat chips accumulate in the erosional pockets, where the currents become slower.

On Mellum Island, the geometry of erosional remnants and pockets has been described by three indices. Those indices define a modification – index [$\text{MOD-I} = I_A \times I_S \times I_N$], which expresses the microbial influence on the morphology of the tidal surface (Noffke & Krumbein, 1999). The variable subindices are: (i) the proportion of mat-covered area related to a defined investigation area ($I_A = A_m/A_i$); (ii) the degree of steepness of slope angles of raised erosional remnants ($I_S = \sin \alpha$); and (iii) the degree of microbial leveling of a rippled sedimentary surface ($I_N = 1 - [(H_p - H_b)/H_p]$). The fossil erosional remnants and pockets show the same geometric dimensions the modern tidal surface morphology. The MOD-I for the fossil examples ranges from 0.12 to 0.68

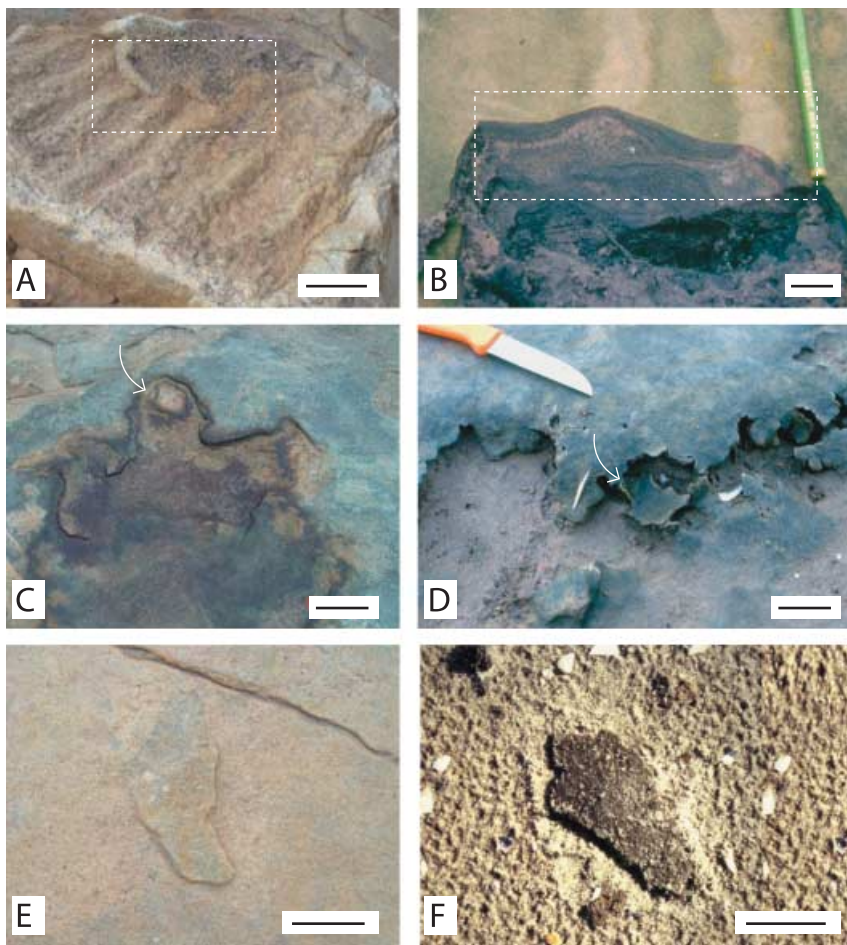


Fig. 6 Subfacies 1: MISS originated by planar microbial mats in the lower supratidal zone of the Nhlazatse Section, Pongola Supergroup; and Recent equivalents. Both the fossil and the modern lower supratidal zones are overgrown by 'epibenthic' microbial mats. This mat type covers its sandy substrate and any sedimentary surface structures like a thick carpet. Therefore, the tidal deposits have a planar (leveled) surface. (A) Rock bed surface in the Nhlazatse Section that shows ripple marks, 'leveled' by an ancient, epibenthic microbial mat; scale: 5 cm. (B) The same view in a modern tidal flat: in vertical section through a mat-covered tidal sand, especially the valleys of former ripple marks are overgrown by a thick microbial mat, and the tidal surface appears even; scale: 2.5 cm; Mellum Island. (C) Fossil erosional remnants and pockets. Arrow: a mat chip of about 2.5 cm in diameter is deposited close to its parent site at the erosional remnant; scale: 4 cm. (D) Actualistic studies on the tidal flats of Mellum Island document that erosional pockets arise from local destruction of a coherent microbial mat by passing bottom water. The mat-covered erosional remnants remain. The erosion takes away pieces of the mat margin, which are redeposited in the erosional pocket (arrow); scale: 2.5 cm. (E) Chip of an ancient microbial mat; scale: 2.5 cm. (F) Chip of a modern microbial mat; scale: 2.5 cm. Note the irregular margin of the chips, which differs from the more rounded margins of mud chips.

(Fig. 7). The MOD-I for equivalent lower supratidal zones on Mellum Island is 0.1 for winter conditions, and 0.60 for summer conditions. Although the measurements conducted on Recent tidal flats document variation of the indices with the seasons, no conclusion can be drawn on seasonality of the Archean climate.

Gas domes. In the lower supratidal zone preserved in the Nhlazatse succession, one widely exposed bedding plane three domlike (Fig. 8). The elevations are round shaped at their basis, and conjoin towards the top. The largest elevation is of 30 cm in diameter at its base, and of 3 cm height. The two smaller ones are 3 and 4 cm wide, and 0.5 and 1 cm high, respectively. The bedding plane is planar (with the exception of the elevations), and shows no ripple marks. Therefore, we interpret those three elevations as ancient gas domes, and not as physically derived sedimentary structures. However, we could not sample the structures in order to search for internal veins or hollows, which, as we know from modern examples, would be characteristic for gas domes.

In modern lower supratidal environments, gas domes are common features that derive from thick microbial mats

sealing the surfaces of the tidal deposits. Such gas domes develop for example on Mellum Island, especially in tidal areas, which are overgrown by the EPS-rich mats of *Microcoleus chthonoplastes*. The mucilages of those microbial mats prohibit the exchange of gases between the tidal deposits and the water or atmosphere, and in consequence intrasedimentary gases accumulate underneath the sealing mat cover. The increasing gas pressure generates hollows within the sediment, and characteristically the vertical section through a Recent gas dome displays a hollow cavern of 1–3 cm length. Gas chromatography showed that those hollows are filled by gases such as H_2S , H_2 , CO, CO_2 and others, mostly deriving from decay of organic matter within the tidal deposits (Noffke, 1997). Typically, the gas domes are located along the normal high water line, so most likely the rising flood tide pushes the intrasedimentary gases upward until the microbial mat domes up. The sizes of the modern gas domes correspond to the dimensions of the fossil examples from the Nhlazatse outcrop. Because sandstones do not usually experience high degrees of compaction during lithification, the preserved shapes of the fossil gas domes should correspond more or less to the original sizes.



Fig. 7 Fossil erosional remnants and pockets in the Nhlazatse Section, Pongola Supergroup, South Africa. 1 Erosional pocket; 2 erosional pocket of which the former mat cover has been flipped over; 3 desiccation crack; 4 wrinkle structure indicating the microbial mat cover on the erosional remnant. The erosional pockets indicate a palaeocurrent from the SW. The modification index of this erosional remnant and pocket structure is $MOD-I = 0.68$. This index corresponds to values of modern microbial mat-covered tidal flats on Mellum Island (0.6 for summer conditions; 0.55 for the yearly average). In the modern tidal flats, currents of about $0.60\text{--}0.75\text{ m s}^{-1}$ would be necessary to give rise to such erosional pockets (microbial mat dominated by cyanobacterium *Microcoleus chthonoplastes*); scale: 25 cm.

Oriented grains. Possible evidence of ancient EPS is apparent in the fine-grained matrix, which contains significant amounts of silica cement of 5–40%. This is a higher content than in the sandstone layers in between the degraded-mat layers (1–15%). In the matrix, single, isolated quartz grains float without any contact to each other (Fig. 9A). This texture, known as ‘orientated grains’, has been shown to be indicative of modern and ancient microbial mats, Fig. 9B (Noffke *et al.*, 1997, 2003b, 2006b). In modern microbial mats, the floating grains originally derived from the substrate. Over time, the particles

are pushed upward and away from each other by the developing biofilms enveloping each grain. Finally, the grains float in the organic matrix without grain-to-grain contact once a complete mat is developed (Fig. 9C). In modern microbial mats, orientated grains are typical features of EPS-rich mats constructed by *Microcoleus chthonoplastes*, but this texture cannot be observed in EPS-poor endobenthic microbial mats built by, for example, *Oscillatoria limosa*. For these reasons, we conclude that the fossil epibenthic microbial mats in the Nhlazatse Section most likely were rich in EPS.

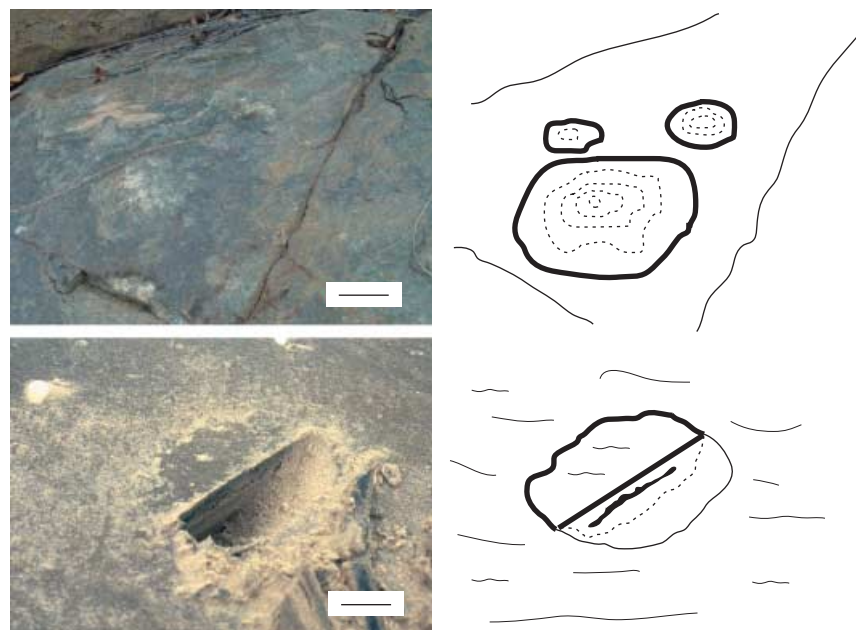


Fig. 8 Fossil and modern gas domes. (A) Gas domes on a well-preserved bedding plane in the Nhlazatse Section, Pongola Supergroup, South Africa (epibenthic microbial mat). (B) Modern gas dome from Mellum Island. In vertical section, a hollow cavern is visible. Here gases are entrapped beneath the EPS-rich microbial mat. Both fossil and modern gas domes occur along the high water line; scales: 5 cm.

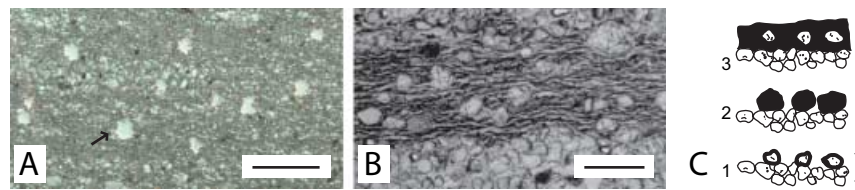


Fig. 9 Microscopic orientated grains are visible in thin-sections of microbial mat laminae. (A) Sandstones of the Nhlazatse outcrop, Pongola Supergroup, show microbial mat laminae that include bigger quartz particles (arrow). Those particles do not have grain-to-grain contact; scale: 500 μm . (B) In modern microbial mats, such textures are termed 'orientated grains', and are common features in epibenthic microbial mats; scale: 500 μm ; Mellum Island. (C) The texture of orientated grains is the result of the growth of a microbial mat: an initial biofilm envelopes the sand particles of a tidal surface; over time the biofilm of each grain grows, pushes the grain upward and away from the surrounding grains; scale: about 0.5 cm (after: Noffke *et al.*, 2001a).

Whereas erosional remnants and pockets, gas domes, and orientated grains indicate the former existence of microbial mats, the supratidal sandstones rarely contain the wavy-crinkly textures that could represent degraded mat fabrics. The reason for the lack of such textures could be intensive recrystallization of the silica and dissolution of organic matter in the course of decay of the water-rich EPS (e.g. Krumbein, 1979; Knoll *et al.*, 1988; Beveridge, 1989; Urrutia & Beveridge, 1993b; Schulze-Lam *et al.*, 1996; Konhauser *et al.*, 2003; also review by Douglas & Beveridge, 1998; Noffke, 2000; Noffke *et al.*, 2001a; Maliva *et al.*, 2005). Thin sections reveal dark, laterally discontinuous laminae (Fig. 10A) that differ in shape and orientation from those of degraded microbial mat features. So these features may document structural reactivation under tectonic pressure, and thus represent stylolites, not microbial mats. Microprobe and microRaman analyses document that clay minerals and organic residuum were collected at low-pressure sites along those stylolites (Fig. 10B). In thin-section,

a second generation of stylolites, less prominent, of grey colour, and composed primarily of chlorite, can be recognized (Fig. 10A). The grey laminae are orientated about 45° to the dark laminae, and could be the result of a second pressure overprint. Structural strain could preferentially affect these layers in which the few sand grains have no grain-to-grain contact because of the ductile response of the matrix. Given their orientation, continuity and composition, these could well also be incipient tectonic fabric (schistosity or cleavage) rather than stylolites.

Subfacies 2: Tufted microbial mats

The Nhlazatse Section also records higher areas of the supratidal zone. Here, tufted microbial mats grew and reached thicknesses of 2–4 cm (Fig. 11A). The tufts are mostly flattened due to loading pressure, and only rarely do upper bedding surfaces display vertically preserved peaks. The vertical preservation is a consequence of fast cementation that sets in

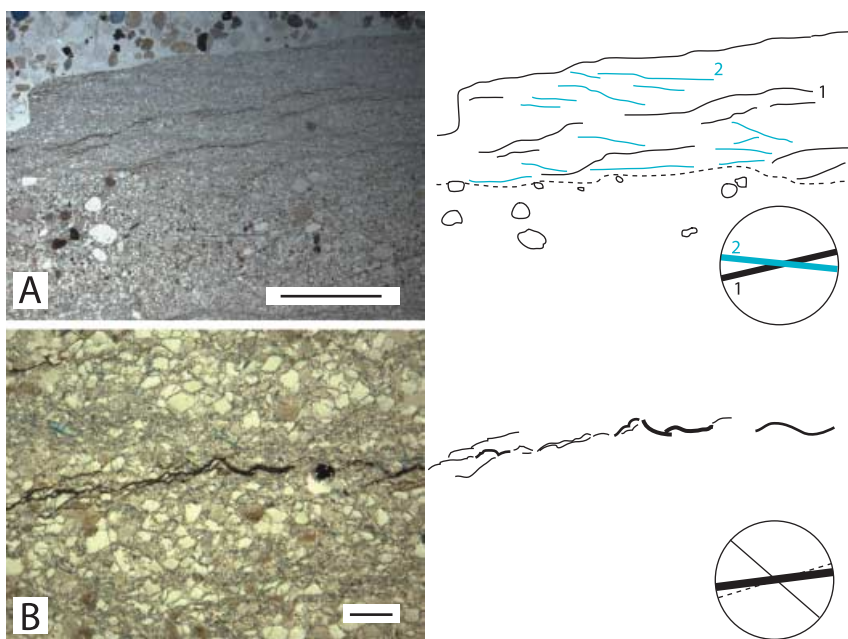


Fig. 10 Stylolites resembling filaments in ancient microbial mats from sandstones of the Nhlazatse Section, lower supratidal zone; thin-sections. (A) In vertical section through an erosional remnant, two groups (1 and 2) of laterally discontinuous laminae are visible. Group 1 consists of clay minerals and organic residuum, group 2 is composed of clay minerals mostly recrystallized to mica. The two groups of laminae are in angle of 15° to each other; scale: 1 cm. (B) Magnification reveals that the laminae show filament-like textures, however, the two groups of laminae are interpreted as stylolites formed by tectonic overprint. The reason for this interpretation is the wide range in thicknesses of the filament-like textures and that the 'filaments' thin out; some filament-like textures bend only around grains, but they are not bent, themselves. The filament-like textures are orientated in a plane, and do not form the characteristic mat fabrics (compare Fig. 6). The organic residuum enriched in the stylolites 1 may have derived from the microbial mat originally creating the erosional remnant; scale: 100 μm .

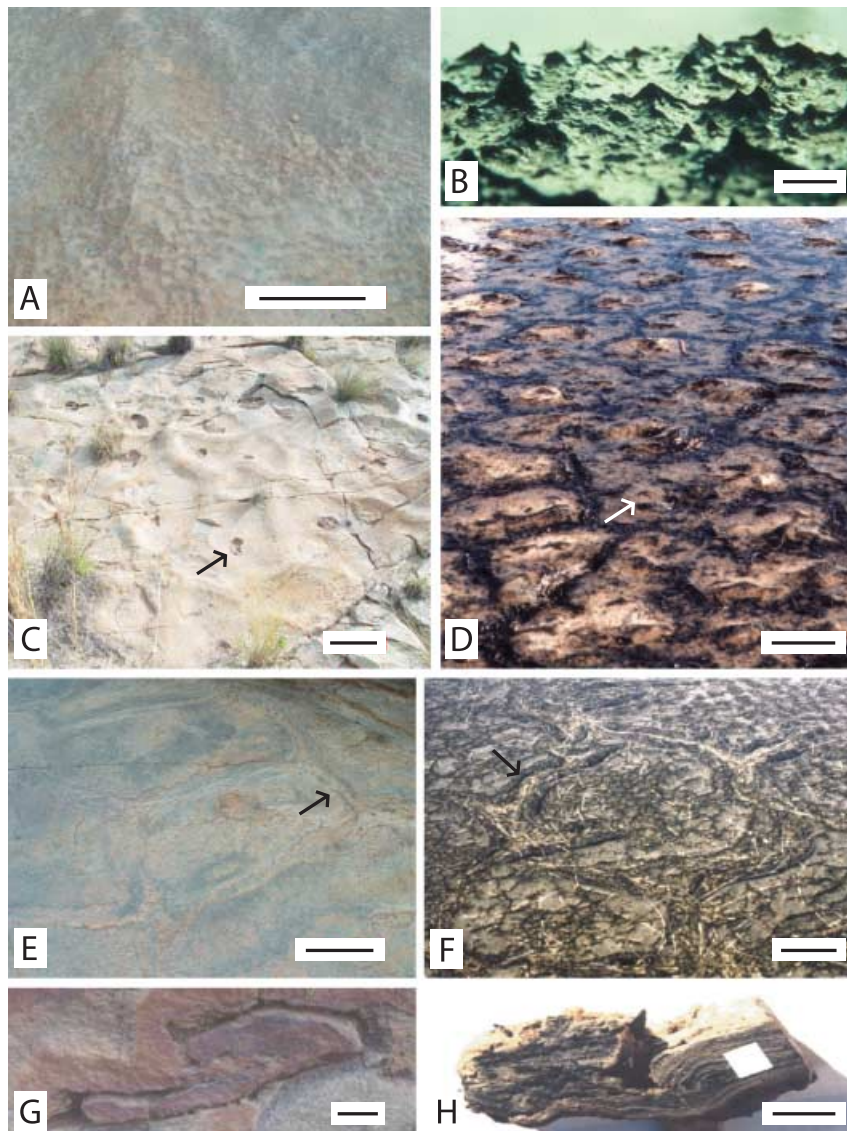


Fig. 11 Subfacies 2: MISS originated by tufted microbial mats in the lower supratidal zone of the Nhlazatse Section, Pongola Supergroup, and modern equivalents from tidal flats of southern Tunisia. (A) In the Nhlazatse Section, many upper bedding planes are planar, and several spotted by tiny pin-like elevations of up to 3 mm height; scale: 10 cm. (B) The magnified surface of a modern microbial mat at the Mediterranean coast reveals that the pin-like elevations are constructed from bundles of vertically orientated cyanobacterial filaments (mainly *Oscillatoria limosa*, *Microcoleus chthonoplastes*, *Lyngbya aestuarii*). Such 'tufts' reach heights of about 2 cm; scale: 1.5 cm. (C) In the Nhlazatse outcrop, polygons of 20–40 cm in diameter cover the ancient tidal surface. In the center of each polygon, a hole a few centimeter in diameter and up to 3 cm depth is visible (arrow). The holes have sharp margins; scale: 25 cm. (D) In the equivalent modern tidal flats, such polygons result from desiccation of a microbial mat during longer lasting dry weather conditions of at least 2 weeks. The holes that form in the center of each polygon are collapsed gas domes. The center of each polygon domes up, because gases of decaying organic matter accumulate underneath the microbial mat. Gas domes up to 20 cm height and 40 cm diameter arise. Later, those gas domes collapse, and the gas escapes through a star-like opening in the roof of the gas dome. Finally, a hole is left behind (arrow). Sometimes the roofs of the gas domes are preserved in the holes; scale: 20 cm. (E) One bedding plane in the Nhlazatse Section displays an *in situ* lithified microbial mat that shows beautifully preserved oscillation cracks. Note the two parallel lines that define the two polygons in this photograph (arrow); scale: 10 cm. (F) The surface of the modern microbial mats at the Tunisian coast display the same oscillation cracks. Note the two parallel bulges (arrow) that are characteristic for this type of crack (compare Fig. 12); scale: 10 cm. (G) Overfolded clast in a sandstone bed (cross-section); scale: 5 cm. (H) Overfolded clast of a thick microbial mat deposited after a storm on the tidal flats of Tunisia. A similar origin of the fossil mat clast shown in (G) is assumed; scale: 5 cm.

during the lifetime of the microbial mats (Kah & Knoll, 1996). Today, we can observe similar microbial mats of similar thicknesses in equivalent positions on the tidal flats of Tunisia (Noffke *et al.*, 2001a). In close-up, the tufts of modern

microbial mats are up to 2 cm high with triangular peaks projecting up from the mat surface Fig. 11B (Gerdes *et al.*, 2000). The tufts are bundles of vertically orientated filaments predominantly of the cyanobacterial species *Microcoleus*

chthonoplastes, *Oscillatoria limosa*, and *Lyngbya aestuarii*. The reason for the formation of these vertical structures is debated. Most probably, the filaments move vertically along each other in order to gain access to light (e.g. Park, 1976; Gerdes *et al.*, 1991, 2000; Kruschel & Castenholz, 1998; Browne *et al.*, 2000; Sumner, 2000; Gerdes & Klenke, 2003).

In the Nhlazatse Section, the bedding surfaces that are marked by tufts also display decimeter-scale patterns of polygons defined by oscillation cracks. Large microbial mat clasts are common as well.

Patterns of polygons. Thirty-one upper bedding planes are covered by up to 100 polygons, each about 20–40 cm in diameter (Fig. 11C). In the center of each polygon, a sharp-margined hole of about 5–10 cm in diameter, and 0.5–3 cm depth is visible (Fig. 11C,D).

This pattern of polygons and holes is characteristic of modern microbial mats in southern Tunisia (Gerdes *et al.*, 2000; Noffke *et al.*, 2001a).

The holes arise from gas domes that form during periods of desiccation of at least 2 weeks. During such arid periods, the decay of organic matter causes gases (mainly CO₂, H₂S, methane, and others) that dome up the center of each polygon. The resulting gas domes reach heights of up to 20 cm. Finally, the tips of the gas domes rupture, the gas escapes, and the gas domes collapse leaving behind a hole in the center of each polygon.

Oscillation cracks. The formation of gas domes is directly related to the formation of the polygons. The polygons are separated from each other by 5- to 10-cm-wide cracks (Fig. 11E,F). The cracks are defined by two parallel ridges of 0.5–2 cm elevation that line the margins of each polygon. In modern Tunisian mats, these cracks have been termed ‘oscillation cracks’ (Noffke *et al.*, 2001a), because they rise from the shrinkage and expansion of each mat polygon in response to the upheaval (and subsequent collapse) of the gas dome in the center. This shrinkage and expansion causes the margins of the mat polygons to roll up, and the ridges are formed. Indeed, the vertical section through a ridge shows the overfolded mat laminae (Fig. 12). Similar bent, lobed laminae are visible in a weathered cross-section of a fossil microbial mat (Fig. 12).

Microbial mat clasts. If the dry weather at the Tunisian study site conditions persists, the microbial mat polygons become brittle, and they loosen like pieces of cracked pavement. If such a desiccated microbial mat is suddenly inundated by water, for example from a storm surge, the microbial mat polygons become eroded. On the tidal flats in Tunisia, the pieces float across the depositional surface, and become deposited at random as allochthonous, large clasts. Many of these are thick and folded (Fig. 11H). In the Nhlazatse Section, similar clasts of up to 40 cm in diameter and 2–4 cm thickness are widespread. Some are overfolded as well, indicating that the original material composing the clasts was ductile and coherent (Fig. 11G). The fossil oscillation cracks and the thick clasts in the Nhlazatse Section may thus document a Mid-Archean climate of alternating humid and arid periods, with episodic flash floods.

Optical and geochemical analyses on the petrological characteristics of the fossil microbial mats of this subfacies 2 show that the lithology is comparable to that of the planar microbial mats of subfacies 1. The ancient tufted microbial mats probably were rich in EPS, similar to the equivalent Tunisian examples today.

Subfacies 3: Microbial mats with spongy fabrics

Six sandstone beds in the Nhlazatse Section contain dark-coloured and coarser-grained lenses of haematite-bound sand (Fig. 13A). The grain size of the sand is medium to coarse, and quartz dominates. The lenses are 0.5–3 m in diameter and about the same thickness (20 cm) as the surrounding beds. The lenses are interpreted as tidal pools where thick and spongy microbial mats developed. In some examples, erosion by passing bottom currents flipped over the microbial mats so their spongy internal fabrics became visible (Fig. 13B).

Modern examples of such mat-overgrown pools include the algal swamps on Andros Island, Bahamas (Hardie, 1978). These have spongy fabrics developed in *Scytonema* mats (Fig. 13C).

DISCUSSION

The Nhlazatse Section of the Sinqueni Formation, Pongola Supergroup, displays a wide array of exceptionally well-preserved

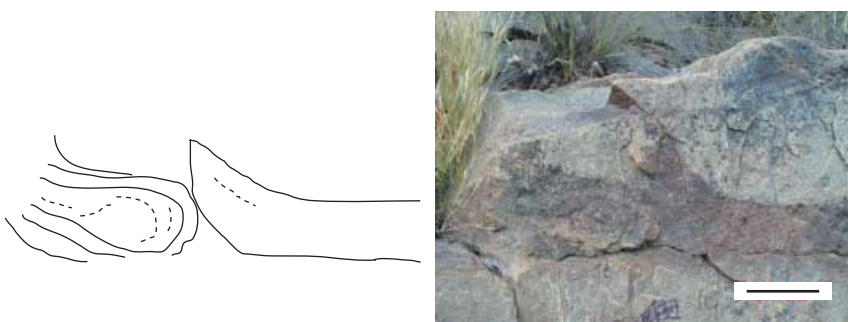


Fig. 12 Oscillation crack in cross-section, preserved in the Nhlazatse succession, Pongola Supergroup. The fossil microbial mat laminae (sketch; left) are overfolded, which gives rise to the ridges along the margins of the polygons; scale: 5 cm.

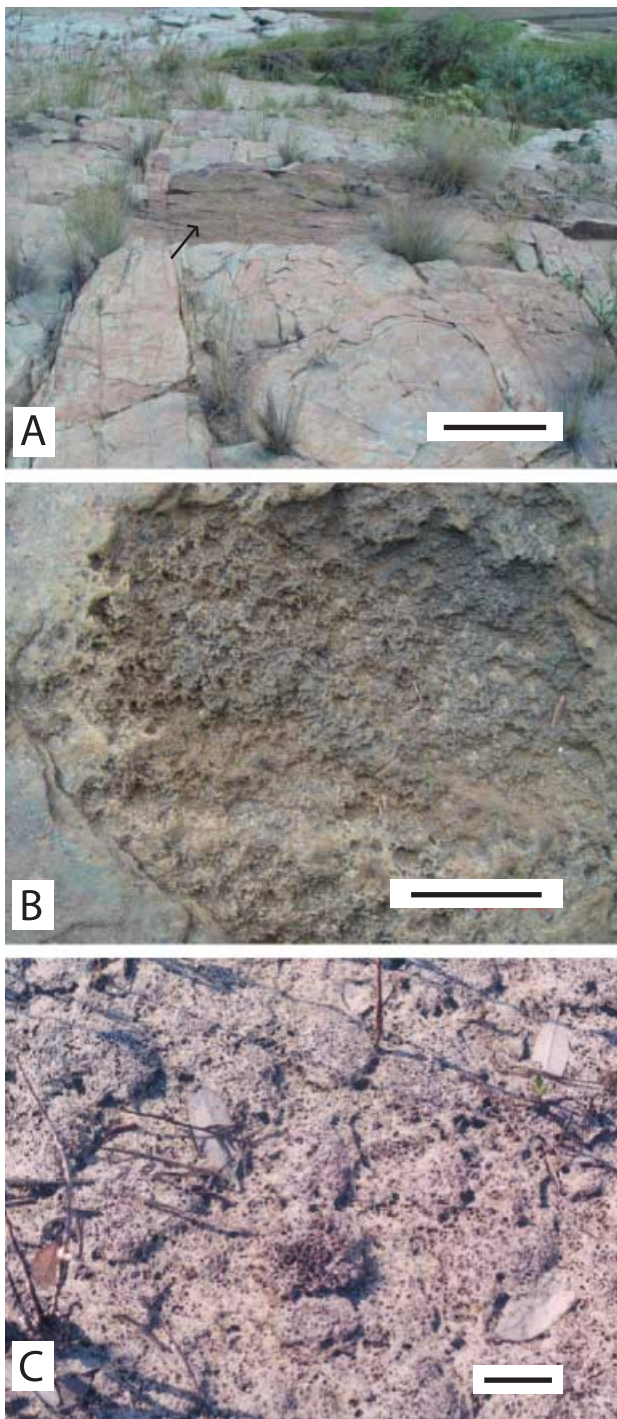


Fig. 13 Subfacies 3: MISS originated by spongy microbial mats in tidal pools of the lower supratidal zone of the Nhlazatse Section, Pongola Supergroup. Modern equivalents from Andros Island, Bahamas. (A) View of an ancient tidal pool (arrow), which had been overgrown by thick and spongy microbial mats. The tidal pools range in sizes from 0.5 to 3 m in diameter and must have been at least 20 cm deep (= thickness of hosting sandstone beds); scale: 1 m. (B) In close-up, the spongy internal texture of the microbial mats is visible; scale: 2.5 cm. (C) Modern *Scytonema* mats in the algal swamps of Andros Island, Bahamas; scale: 5 cm.

MISS. The various structures are specific to different tidal zones, and in thin-sections display textures that can be interpreted as degraded microbial mats. Today, in modern tidal flats, we can observe the same MISS with an equivalent distribution relative to the main tidal zones. The MISS of the Nhlazatse section correspond in geometries and dimensions to the modern MISS. As the modern MISS are constructed by cyanobacterial mats, these findings are not inconsistent with the presence of cyanobacteria 2.9 Ga ago. Because Beukes & Lowe (1989) regard contemporaneous, carbonate stromatolites in the Pongola Supergroup as potentially produced by benthic cyanobacteria, the occurrence of this bacterial group in siliclastic settings would not be a surprise. However, the age of the earliest cyanobacteria is under debate (e.g. Knoll, 1999; Olson, 2006). Many objects resembling bacterial fossils have been reported as possible cyanobacteria (e.g. Klein *et al.*, 1987, from the 2.3–2.6 Transvaal Supergroup, South Africa; Altermann & Schopf, 1995, from the 2.6-Ga-old Campbellrand Group, South Africa; Kazmierczak & Altermann, 2002, from the 2.6-Ga-old Nauga Formation, South Africa). Some may be correctly interpreted, but definitive diagnostic evidence prior to 2.7 Ga is lacking. A strong case for Meso-Archean (2.7–2.8 Ga) cyanobacteria is provided by the 2Me-hopanoid data of Brocks *et al.* (1999), although the question of whether these biomarkers are diagnostic for crown-group cyanobacteria with two photosystems is unresolved. Buick (1992) described 2.7-Ga-old stromatolites in an ancient sulfate-deficient lake environment from the Tumbiana Formation, Fortescue Group, Australia, which imply that oxygenic photosynthesis was the principal carbon-fixing metabolism. So while the presence of cyanobacteria older than ~2.7 Ga cannot be conclusively demonstrated, our results for the Meso-Archean sandstones could potentially point to an extended history for this microbial group. The results correspond to our earlier observations based on studies of siliclastic rock successions of the roughly contemporaneous Ntombe Formation, Pongola Supergroup, and the Brixton Formation, Witwatersrand Supergroup (Noffke *et al.*, 2003b, 2006a). Taken together, all sandstone successions record temporally and spatially widespread MISS distributed across the ancient photic zone. Their structures indicate that photoautotrophic microbial mats effectively stabilized the sandy substrata. While the MISS in the Nhlazatse Section are consistent with cyanobacterial activity, it should be noted that there are noncyanobacterial mat-forming phototrophic microbes of similar size and shape that could also have produced such structures. However, such structures have not been described from modern settings. In modern environments, the photoautotrophic green sulfur bacteria, heliobacteria, and chloroflexi have representatives with mobile filaments that under specific conditions may construct sediment-stabilizing mat fabrics. Non-photoautotrophic, sulphur-oxidizing bacteria also form mats in deep-water settings (e.g. Williams & Reimers, 1983), but may have done so elsewhere in the Archean. Flexibacteria with mobile filaments

are widespread in modern marine settings, and may contribute to microbial mats in some settings (e.g. Mattison *et al.*, 1998).

In summary, the Nhlazatse Section displays spectacular biogenic structures, and offers the opportunity for an actualistic comparison between today's microbial mats and the Archean world 2.9 Ga old. The study shows that independent from stromatolites or microfossils, MISS are valuable tools for the investigation of early life. We would like to call for the conservation of this unique type location in the Wit Mfolozi River Gorge to provide a forum for future scientific studies.

ACKNOWLEDGEMENTS

This contribution greatly benefited from discussions with Roger Buick and Andrew H. Knoll, as well as from the reviews. We thank the NASA Exobiology Program, the NASA Mars Fundamental Research Program, the NASA Astrobiology Institute, and the Carnegie Institution of Washington DC for the funding of this study. Technical assistance was provided by Marilyn Fogel and Chris Hadidiacos.

REFERENCES

- Altermann W, Kazmierczak J (2003) Archean microfossils: a reappraisal of early life on Earth. *Research in Microbiology* **154**, 611–617.
- Altermann W, Schopf JW (1995) Microfossils from the Neoproterozoic Campbell Group, Griqualand West Sequence of the Transvaal Supergroup, and their paleoenvironmental and evolutionary implications. *Precambrian Research* **75**, 65–90.
- Awramik SM, Schopf J, Walter MR (1983) Filamentous fossil bacteria from the Archean of Western Australia. *Precambrian Research* **20**, 357–374.
- Beukes NJ (1996) Sole Marks and combined-flow storm event beds in the Brixton Formation of the siliciclastic Archean Witwatersrand Supergroup, South Africa. *Journal of Sedimentary Research* **66**, 567–576.
- Beukes NJ, Cairncross B (1991) A lithostratigraphic-sedimentological reference profile for the late Mozaan Group, Pongola Sequence: Application to sequence stratigraphy and correlation with the Witwatersrand Supergroup. *South African Journal of Geology* **94**, 44–69.
- Beukes NJ, Lowe DR (1989) Environmental control on diverse stromatolite morphologies in the 3000 Myr Pongola Supergroup, South Africa. *Sedimentology* **36**, 383–397.
- Beukes NJ, Eriksson E, Sumner DY (2002) *Archean to Proterozoic Sedimentological Superlatives along the Eastern Kaapvaal Craton*. Excursion Guide, 16th International Conference, Rand Afrikaans University, South Africa, 79 pp.
- Beveridge TJ (1989) Role of cellular design in bacterial metal accumulation and mineralization. *Annual Reviews Microbiology* **43**, 147–171.
- Bland BH (1984) Arumberia Glaessner & Walter, a review of its potential for correlation in the region of the Precambrian Cambrian boundary. *Geological Magazine* **121**, 625–633.
- Bottjer DJ (2005) Geobiology and the fossil record: eukaryotes, microbes, and their interactions. In *Geobiology: Objectives, Concepts, Perspectives* (ed. Noffke N). Elsevier, Amsterdam, pp. 5–22.
- Boyce CK, Hazen RM, Knoll AH (2001) Nondestructive, in situ, cellular-scale mapping of elemental abundances including organic carbon in permineralized fossils. *Proceedings of the National Academy of Sciences of the USA* **98**, 5970–5974.
- Brasier MD, Green OR, Jephcoat AP, Klepepe AK, Van Kranendonk MJ, Lindsay JF, Steele A, Grasslmeau MV (2002) Questioning the evidence for Earth's oldest fossils. *Nature* **416**, 76–91.
- Brasier MD, Green OR, Lindsay JF, McLoughlin N, Steele A, Stoakes C (2005) Critical testing of Earth's oldest putative fossil assemblage from the ~3.5 Ga Apex chert, Chinaman Creek, Western Australia. *Precambrian Research* **140**, 55–102.
- Brasier MD, McLoughlin N, Green O, Wacey D (2006) A fresh look at the fossil evidence for early Archean cellular life. *Philosophical Transactions of the Royal Society of London. Series B, Biological Sciences* **361**, 887–902.
- Brocks JJ, Logan GA, Buick R, Summons EE (1999) Archean molecular fossils and the early rise of eukaryotes. *Science* **285**, 1033–1036.
- Browne KM, Golubic S, Seong-Joo L (2000) Shallow-marine microbial carbonate deposits. In *Microbial Sediments* (eds Riding R, Awramik S). Springer, Berlin, pp. 233–249.
- Buick R (1990) Microfossil recognition in Archean rocks: an appraisal of spheroids and filaments from 3500 MY old chert-barite at North Pole, Western Australia. *Palaio* **5**, 441–459.
- Buick R (1992) The antiquity of oxygenic photosynthesis: evidence from stromatolites in sulfate-deficient Archean lakes. *Science* **255**, 74–77.
- Buick R (2001) Life in the Archean. In *Paleobiology II* (eds Briggs DG, Crowther PR). Blackwell Science, Oxford, pp. 13–21.
- Buick R, Dunlop JS, Groves DJ (1981) Stromatolite recognition in ancient rocks: an appraisal of irregularly laminated structures in early Archean chert-barite unit from North Pole, Western Australia. *Alcheringa* **5**, 161–181.
- Decho AW (1990) Microbial exopolymer secretions in ocean environments: their role(s) in food webs and marine processes. *Oceanographic and Marine Biology. Annual Review* **28**, 73–154.
- Douglas S, Beveridge TJ (1998) Mineral formation by bacteria in natural microbial communities. *Microbial Ecology* **26**, 79–88.
- Faure G, Mensing TA (2004) *Isotopes: Principles and Applications*. John Wiley, New York.
- Gehling JG (1982) The sedimentology and stratigraphy of the Precambrian Pound Subgroup, Central Flinders Ranges, South Australia. MSc Dissertation, University of Adelaide, Adelaide, SA, Australia, pp. 1–112.
- Gehling JG (1999) Microbial mats in terminal Proterozoic siliciclastics: Ediacaran death masks. *Palaio* **14**, 40–57.
- Gehling JG (2000) Environmental interpretation and a sequence stratigraphic framework for the terminal Proterozoic Ediacara member within the Rawnsley Quartzite, South Australia. *Precambrian Research* **100**, 65–95.
- Gerdes G, Klenke T (2003) Geologische Bedeutung oekologischer Zeitraume in biogener Schichtung (Mikrobenmatten, potentielle Stromatolithe). *Mitt Ges Geological Bergbaustud Oesterreich* **46**, 35–49.
- Gerdes G, Krumbein WE, Reineck HE (1991) Biolaminations – ecological versus depositional dynamics. In: *Cycles and Events in Stratigraphy* (eds Einsele, G, Ricken, W, Seilacher, A). Springer, Berlin, pp. 592–607.
- Gerdes G, Claes M, Dunajtschik-Piewak K, Riege H, Krumbein WE, Reineck HE (1993) Contribution of microbial mats to sedimentary surface structures. *Facies* **29**, 61–74.
- Gerdes G, Noffke N, Klenke T, Krumbein WE (2000) Microbial signatures in peritidal sediments – A catalogue. *Sedimentology* **47**, 279–308.
- Golubic SG, Knoll AH (1999) Prokaryotes. In *Fossil Prokaryotes and Protists* (ed. Lipps J). Blackwell, Boston, Massachusetts, pp. 51–76.

- Grotzinger JP, Knoll AH (1999) Stromatolites in Precambrian carbonates: evolutionary mileposts or environmental dipsticks? *Annual Review of Earth and Planetary Science* **27**, 313–358.
- Grotzinger JP, Rothman DH (1996) An abiotic model for stromatolite morphogenesis. *Nature* **383**, 423–425.
- Hagadorn JW, Bottjer DJ (1997) Wrinkle structures: microbially mediated sedimentary structures in siliciclastic settings at the Proterozoic–Phanerozoic transition. *Geology* **25**, 1047–1050.
- Hagadorn JW, Bottjer DJ (1999) Unexplored microbial worlds. *Palaio* **14**, 1–93.
- Hardie LA (1978) *Sedimentation on the Modern Tidal Flats of Northwest Andros Island, Bahamas*. Johns Hopkins University Press, Baltimore, Maryland.
- Hofmann HJ, Grey K, Hickman AH, Thorpe RI (1999) Origin of 3.45 Ga coniform stromatolites in the Warawoona Group, Western Australia. *Geological Society of America Bulletin* **111**, 1256–1262.
- Kah LC, Knoll AH (1996) Microbenthic distribution of Proterozoic tidal flats: environmental and taphonomic considerations. *Geology* **24**, 79–82.
- Kazmierczak J, Altermann W (2002) Neoproterozoic biomineralization by benthic cyanobacteria. *Science* **298**, 2351.
- Klein C, Beukes NJ, Schopf JW (1987) Filamentous microfossils in the early Proterozoic Transvaal Supergroup: their morphology, significance, and paleoenvironmental setting. *Precambrian Research* **36**, 81–94.
- Knoll AH (1999) A new window into evolution. *Science* **285**, 1025–1026.
- Knoll AH (2003) *Life on a Young Planet*. Princeton University Press, Princeton.
- Knoll AH, Barghoorn ES (1977) Archean microfossils showing cell division from the Swaziland System of South Africa. *Science* **198**, 396–398.
- Knoll AH, Strother P, Rossi S (1988) Distribution and diagenesis of silicified microfossils from the Lower Proterozoic Duck Creek Formation, Western Australia. *Precambrian Research* **38**, 257–279.
- Konhauser KO, Jones B, Reysenbach AL, Renault RW (2003) Hot spring sinters: key to understanding Earth's earliest life forms. *Canadian Journal of Earth Science* **40**, 1713–1724.
- Krumbein WE (1979) Photolithotrophic and chemoorganotrophic activity of bacteria and algae as related to beachrock formation and degradation (Gulf of Aquaba, Sinai). *Geomicrobiology Journal* **1**, 156–202.
- Kruschel C, Castenholz RW (1998) The effect of solar UV and visible irradiance on the vertical movements of cyanobacteria in microbial mats. *FEMS Microbiology Ecology* **27**, 53–72.
- Lowe DR (1980) Stromatolites 3.4000–Myr old from the Archean of Western Australia. *Nature* **284**, 441–443.
- Lowe DR (1994) Abiological origin of described stromatolites older than 3.2 Ga. *Geology* **22**, 387–390.
- Maliva R, Knoll AH, Simonson B (2005) Secular change in the Precambrian silica cycle: insights from chert petrology. *Bulletin Geological Society of America* **117**, 835–845.
- Matthews PE (1967) The pre-Karoo formations of the White Umfolozi inlier, northern Natal. Geological Society of South Africa, Transactions, 70.
- Mattison R, Abbiati M, Dando P, Fitzsimons M, Pratt S, Southward A, Southward E (1998) Chemoautotrophic microbial mats in submarine caves with hydrothermal sulphidic springs at Cape Palinuro, Italy. *Microbial Ecology* **35**, 58–71.
- Noffke N (1997) Mikrobiell induzierte Sedimentstrukturen (M.I.S.S.) in siliziklastischen Wattablagerungen. PhD Thesis University of Oldenburg, Oldenburg, Germany, 127 p.
- Noffke N (1998) Multidirected ripple marks rising from biological and sedimentological processes in modern lower supratidal deposits (Mellum Island, southern North Sea). *Geology* **26**, 879–882.
- Noffke N (1999) Erosional remnants and pockets evolving from biotic–physical interactions in a Recent lower supratidal environment. *Sedimentary Geology* **123**, 175–181.
- Noffke N (2000) Extensive microbial mats and their influences on the erosional and depositional dynamics of a siliciclastic cold water environment (lower Arenigian, Montagne Noire, France). *Sedimentary Geology* **136**, 207–215.
- Noffke N, Krumbein WE (1999) A quantitative approach to sedimentary surface structures contoured by the interplay of microbial colonization and physical dynamics. *Sedimentology* **46**, 417–426.
- Noffke N, Gerdes G, Klenke T, Krumbein WE (1997) A microscopic sedimentary succession indicating the presence of microbial mats in siliciclastic tidal flats. *Sedimentary Geology* **110**, 1–6.
- Noffke N, Gerdes G, Klenke T, Krumbein WE (2001a) Microbially induced sedimentary structures indicating climatological, hydrological and depositional conditions within Recent and Pleistocene coastal facies zones (southern Tunisia). *Facies* **44**, 23–30.
- Noffke N, Gerdes G, Klenke T, Krumbein WE (2001b) Microbially induced sedimentary structures – A new category within the classification of primary sedimentary structures. *Journal of Sedimentary Research* **71**, 649–656.
- Noffke N, Knoll AH, Grotzinger J (2002) Sedimentary controls on the formation and preservation of microbial mats in siliciclastic deposits: a case study from the upper Neoproterozoic Nama Group. *Namibia Palaio* **17**, 1–14.
- Noffke N, Beukes NJ, Hazen RM (2006a) Microbially induced sedimentary structures in the 2.9 Ga old Brixton Formation, Witwatersrand Supergroup, South Africa. *Precambrian Research* **146**, 35–44.
- Noffke N, Hazen RM, Eriksson K, Simpson E (2006b) A new window into early life: Microbial mats in a siliciclastic early Archean tidal flat (3.2 Ga Moodies Group, South Africa). *Geology* **34**, 253–256.
- Noffke N, Gerdes G, Klenke T (2003a) Benthic cyanobacteria and their influence on the sedimentary dynamics of peritidal depositional systems (siliciclastic, evaporitic salty and evaporitic carbonatic). *Earth-Science Reviews* **12**, 1–14.
- Noffke N, Hazen RM, Nhlenko N (2003b) Earth's earliest microbial mats in a siliciclastic marine environment (Mozaan Group, 2.9 Ga, South Africa). *Geology* **31**, 673–676.
- Olson JM (2006) Photosynthesis in the Archean era. *Photosynthesis Research* **88**, 109–117.
- Park RA (1976) The preservation potential of some recent stromatolites. *Sedimentology* **24**, 485–506.
- Pflueger F, Gresse P (1996) Microbial sand chips – a non-actualistic sedimentary structure. *Sedimentary Geology* **102**, 263–274.
- Reid RP, Visscher PT, Decho AW, Stolz JF, Bebout BM, Dupraz C, Macintyre IG, Paerl HW, Pinckney JL, Prufert-Bebout L, Stegge TF, DesMarais DJ (2000) The role of microbes in accretion, lamination and early lithification of modern marine stromatolites. *Nature* **406**, 989–991.
- Runnegar BN, Fedonkin MA (1992) Proterozoic metazoan body fossils. In *The Proterozoic Biosphere: A Multidisciplinary Study* (eds Schopf JW, Klein C). Cambridge University Press, New York, pp. 369–387.
- Schidlowski M, Hayes JM, Kaplan IR (1983) Isotopic inferences of ancient biochemistries: Carbon, sulfur, hydrogen and nitrogen. In *Earth's Earliest Biosphere: its Origin and Evolution* (ed. Schopf JW). Princeton University Press, Princeton, New Jersey, pp. 149–186.

- Schieber J (1999) Microbial mats in terrigenous clastics: the challenge of identification in the rock record. In *Unexplored Microbial Worlds* (eds Hagadorn JW, Pflueger F, Bottjer DJ). *Palaios* **14**, 3–13.
- Schieber J (2004) Microbial mats in the siliciclastic rock record: a summary of diagnostic features. In *The Precambrian Earth: Tempos and Events* (eds Eriksson PG, Altermann DR, Nelson DR, Mueller WE, Catuneanu O). Elsevier, Amsterdam, pp. 663–673.
- Schopf JW (1993) Microfossils of the Early Archean Apex chert: new evidence of the antiquity of life. *Science* **260**, 640–646.
- Schopf JW (2006) Fossil evidence of Archaean life. *Philosophical Transactions of the Royal Society of London. Series B, Biological Sciences* **361**, 869–885.
- Schopf JW, Packer BM (1987) Early Archean (3.3-billion to 3.5-billion-year-old) microfossils from Warrawoona Group. *Australia Science* **237**, 70–74.
- Schopf JW, Walter MR (1983) Archean microfossils: new evidence of ancient microbes. In *Earth's Earliest Biosphere: its Origin and Evolution* (ed. Schopf JW). Princeton University Press, Princeton, New Jersey, pp. 214–239.
- Schopf JW, Kudryavtsev AB, Agresti DG, Wdowlak TJ, Czaja AD (2002) Laser-Raman imagery of Earth's earliest fossils. *Nature* **416**, 73–76.
- Schulze-Lam S, Fortin D, Davis BS, Beveridge TJ (1996) Mineralization of bacterial surfaces. *Chemical Geology* **132**, 171–181.
- Shen Y, Buick R, Canfield DE (2001) Isotopic evidence for microbial sulphate reduction in the early Archean era. *Nature* **410**, 77–81.
- Simonson BM, Carney KE (1999) Roll-up structures: evidence of situ microbial mats in Late Archean deep shelf environments. *Palaios* **14**, 13–24.
- Strauss H (2003) Sulphur isotopes and the early Archaean sulphur cycle. *Precambrian Research* **126**, 349–361.
- Summons R, Hope M, Logan GA (1999) 2-Methylhopanoids as biomarkers for cyanobacterial oxygenic photosynthesis. *Nature* **400**, 554–557.
- Sumner DY (2000) Microbial vs environmental influences on the morphology of Late Archean fenestrate microbialites. In *Microbial Sediments* (eds Riding R, Awramik SM). Springer-Verlag, Heidelberg, Germany, pp. 307–314.
- Tice MM, Lowe DR (2004) Photosynthetic microbial mats in the 3.5 Ga old ocean. *Nature* **431**, 549–550.
- Ueno Y, Maruyama S, Isozaki Y, Yurimoto H (2001) Early Archean (ca. 3.5 Ga) microfossils and ¹³C-depleted carbonaceous matter in the North Pole area, Western Australia: field occurrence and geochemistry. In *Geochemistry and the Origin of Life* (eds Nakashima S, Mruyama A, Windley BF). Universal Academy Press, Tokyo, pp. 203–236.
- Urrutia M, Beveridge TJ (1993b) Mechanism of silicate binding to the bacterial cell wall in *Bacillus subtilis*. *Journal of Bacteriology* **175**, 1936–1946.
- Villbrandt M (1992) Interactions of nitrogen fixation and photosynthesis in marine cyanobacterial mats (Mellum, southern North Sea), PhD Thesis University of Oldenburg, Oldenburg, Germany, 153 p.
- Walsh MM, Lowe DR (1985) Filamentous microfossils from the 3500 Myr-old Onverwacht Group, Barberton Mountain Land, South Africa. *Nature* **314**, 530–532.
- Walter MR (1972) Stromatolites and biostratigraphy of the Australian Precambrian and Cambrian. *Paleontological Association of London Special Papers, Paleontology* **11**, 190.
- Walter MR, Buick R, Dunlop JS (1980) Stromatolites, 3.4–3.5 Myr old from the North Pole area, Western Australia. *Nature* **284**, 443–445.
- Westall F, de Wit MJ, Dann M, van der Gaast S, de Ronde CE, Gerneke D (2001) Early Archean fossil bacteria and biofilms in hydrothermally influenced sediment from the Barberton Greenstone Belt, South Africa. *Precambrian Research* **106**, 93–116.
- Williams LA, Reimers C (1983) Role of bacterial mats in oxygen-deficient marine basins and coastal upwelling regimes: preliminary report. *Geology* **11**, 267–269.